

A new approach to characterize grip force applied to a cylindrical handle[☆]

Ren G. Dong^{*}, John Z. Wu, Daniel E. Welcome,
Thomas W. McDowell

*Engineering & Control Technology Branch, National Institute for Occupational Safety and Health,
1095 Willowdale Road, Morgantown, MS L-2027, WV 26505, USA*

Received 21 July 2006; received in revised form 16 January 2007; accepted 20 January 2007

Abstract

The grip force applied to a cylindrical handle is a function of the measurement reference axis. So far, however, no attempt has been made to fully describe the exact form of this function. The objectives of this study were to examine some fundamental characteristics of grip forces and to explore the basic pattern of the grip force function. Twenty subjects (10 males and 10 females) participated in the experiment. The subjects alternately used their left and right hands to apply maximum grip forces and medium grip forces (about 40% of maximum) to a 30 mm handle. A flexible pressure sensor mat was used to measure the grip pressure. The pressure was integrated with respect to different measurement axes; this resulted in the grip force function. This study found that every gripping action produces maximum and minimum force axes; these axes are separated by about 90°. The maximum force is correlated with the minimum force, but the former is generally about 1.42 times the latter. The principal grip direction is about 78° from the z_h -axis of the hand biodynamic coordinate system defined in ISO 8727 [ISO 8727. Mechanical vibration and shock – human exposure – biodynamic coordinate systems. Geneva, Switzerland: International Organization for Standardization; 1997]. More interestingly, each of the 160 sets of experimental data reasonably fit this study's proposed elliptical model. The implications of the findings are discussed.

© 2007 IPPEM. Published by Elsevier Ltd. All rights reserved.

Keywords: Grip force; Grip strength; Hand force; Hand; Grip pressure

1. Introduction

Repeated forceful hand actions in many workplaces have been strongly associated with musculoskeletal disorders (MSDs) of the upper extremities such as carpal tunnel syndrome (CTS), hand/wrist tendonitis, and hand–arm vibration syndrome (HAVS) [2,3]. A comprehensive understanding of hand forces is important for developing appropriate strategies and working procedures geared to reduce these disorders. Orientation relationships of hand forces relative to the hand and arm anatomical structures can provide critical information for determining the forces and stresses acting on

the muscles, joints, and bones of the hand–wrist–arm system. More detailed hand force information is also desired for the development of safer and more efficient hand tools. Unfortunately, although the International Organization for Standardization (ISO) has set forth an international standard, ISO 15230 [4], on hand forces, there has been no consensus as to how to best measure or characterize hand forces. Further studies are required to properly describe and quantify hand forces.

The grip force applied to a cylindrical handle is one of the most important hand force components. As defined in the international standard [4], the grip force is “half the sum of the force components towards an axis inside the handle without push, pull, or lifting forces. Simplified, the grip force is the clamp-like force exerted by the hand of the operator when enclosing the handle.” Ignoring the effect of the tool inertia force, this standard further states “The force is compensated

[☆] The findings and conclusions in this report are those of the authors and do not necessarily represent the views of the National Institute for Occupational Safety and Health.

^{*} Corresponding author. Tel.: +1 304 285 6332; fax: +1 304 285 6265.
E-mail address: rkd6@cdc.gov (R.G. Dong).

within the hand by a grip force acting in the opposite direction towards a dividing plane.”

The maximum voluntary contraction grip force is conventionally termed as grip strength, and it has been frequently used to help diagnose some hand musculoskeletal disorders, to examine the effectiveness of the disorder treatments, and to design tools [3,5–8]. Grip strength is usually measured using an apparatus such as Jamar dynamometer. Such a dynamometer has a geometry that is not representative of cylindrical handles featured on many manual and powered hand tools. Because of such geometrical differences, the grip pressure distribution on a Jamar dynamometer is quite different from that on a cylindrical handle. As a result, the grip strength measured using a Jamar dynamometer may also be different from that measured on a cylindrical handle, although little knowledge regarding these measurement relationships exists. It is thus worthwhile to measure the grip strength on cylindrical handles for optimizing tool designs and for risk assessments of tool operations.

To fully characterize grip forces applied to cylindrical handles, it is essential to know how the grip force can be appropriately described and quantified on such handles. So far, grip forces applied to such handles have been usually measured in a single axis, e.g., [9,10]. This approach has been widely used to monitor and control the grip force during glove tests, biodynamic response measurements, and many other experiments involving hand grip simulations, e.g., [11–13]. This approach has also been adopted in an international standard for glove testing (ISO 10819) [14]. However, on a cylindrical handle, the grip force measured on one axis could be substantially different from that measured on another axis [15]. This brings about two critical questions: which axis should be used to measure grip force? Is the current practice acceptable, or is it biased?

In ISO 15230 [4], it is stated that “When the operator is gripping a cylindrical handle, the direction of the main grip force is generally parallel to the z -axis defined in ISO 8727”. If this holds true, it might be reasonable to use the force measured on the z -axis to represent the grip force. This assertion, however, is doubtful.

Alternatively, a few investigators proposed using a vector as a measure of the grip force [15]. The proposed vector was formed using two force values measured on two specific orthogonal axes on the hand. The physical meaning of such a force vector is unclear. Specifically, it is unclear if the direction of the vector is truly associated with the hand orientation. It is also unclear if the magnitude of the vector is representative of the total grip effort applied to the handle.

The above-described background suggests that the grip force applied to a cylindrical handle is a function of the measurement axis or orientation. This function likely has maximum and minimum values in certain orientations of the hand coordinate system. However, it is unknown whether this function follows any pattern. It is unclear as to which orientation the principal force is positioned. Such knowledge is useful for the designs of tools that require gripping

in a specific orientation, to analyze the forces and stresses inside the hand and arm, and to appropriately monitor and control the applied grip force in experiments requiring gripping actions. Such fundamental knowledge is also required to develop more effective methodologies for measuring the grip force or strength applied to a cylindrical handle. Therefore, the objectives of this study were to further the understanding of the characteristics of grip forces applied to cylindrical handles and to identify the fundamental pattern of grip force as a function of its measurement axis.

2. Methods

2.1. Theoretical analysis

2.1.1. Definition of idealized grip force

According to the definitions and descriptions in ISO 15230 [4], the grip force mainly results from the grip contact pressure normal to the handle surface. It is possible that some friction force tangential to the surface may also contribute to the grip force. The distribution of the friction force in the grip action is neglected in ISO 15230, most likely because it is complicated and difficult to measure. To simplify the current study, the friction force was assumed to be small, and it does not change the basic pattern of the grip force function. Therefore, the idealized grip force used in this study is resulted solely from the grip pressure, as shown in Fig. 1.

For the purpose of this study, the distribution of the grip pressure along the longitudinal direction of the handle is not of concern, but the pressure distribution around the circumference of a cross section of the handle is essential for determining grip force as a function of the measurement axis. Therefore, the pressure along the longitudinal direction is lumped to the circumference of the circle representing the handle. The pressure on each half of the circle can be simplified into an equivalent force vector acting at the center of

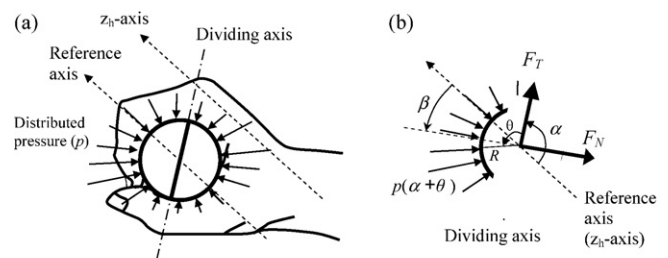


Fig. 1. Graphical views of (a) hand grip pressure distribution and definitions of the various axes, and (b) hand grip pressure (p) per unit length of handle circumference at $\alpha + \theta$ degrees from the reference axis, grip normal force (F_N), and grip tangential force (F_T). In (b), α is the angle of F_T or the moving dividing axis referred to the fixed reference axis (parallel to z_h -axis of the hand biodynamic coordinate system), $\beta (= \alpha - 90^\circ)$ is the angle of F_N measured from the reference axis, θ is a relative angle measured from the dividing axis, and R is the handle radius.

the circle. This vector can be expressed using two orthogonal components: F_N is the normal component (or force perpendicular to the dividing axis or plane); F_T is the tangential component (or force tangential to the dividing plane). The normal component is conventionally termed as ‘grip force’ and exclusively used in previous studies and applications. In the past, the tangential component has been totally ignored. As demonstrated in this study, however, the tangential component can help in characterizing the grip force.

The z_h -axis of the biodynamic hand coordinate system defined in ISO 8727 [1] is included in Fig. 1a, which is defined as the axis that “passes proximally through the origin and is the long axis of the third metacarpal bone.” The axis parallel to the z_h -axis and passing through the center of the handle circle was used as the reference axis for determining the angular position (α) of the circle’s dividing axis. In ISO 5349-1 [16], this axis is also defined as the z_h -axis of the hand biodynamic coordinate system. Referencing the symbols defined in Fig. 1, the two grip force components can be calculated from:

$$\begin{aligned} F_N(\alpha) &= \int_0^\pi p(\alpha + \theta) \sin(\theta) R d\theta, \\ F_T(\alpha) &= \int_0^\pi p(\alpha + \theta) \cos(\theta) R d\theta \end{aligned} \quad (1)$$

2.1.2. Fundamental properties of the idealized grip force

According to the definitions, the idealized grip force on one-half of the handle must be balanced by that on the other half. This can be expressed as follows:

$$F_N(\alpha) = F_N(\alpha + \pi), \quad F_T(\alpha) = F_T(\alpha + \pi) \quad (2)$$

As detailed in Appendix A, we proved from Eq. (1) that

$$\begin{aligned} \frac{dF_N(\alpha)}{d\alpha} &= -F_T(\alpha), \\ \frac{dF_T(\alpha)}{d\alpha} &= -R[p(\alpha + \pi) + p(\alpha)] + F_N(\alpha) \end{aligned} \quad (3)$$

At the maximum and minimum grip normal forces ($F_{N_{\max}}$ and $F_{N_{\min}}$), the derivative of the grip normal force ($dF_N/d\alpha$) must be equal to zero; therefore, according to Eq. (3), the tangential force is equal to zero at the orientations of such normal forces. In this study, the maximum and minimum grip normal forces were termed as the first principal grip force (F_1) and the second principal grip normal force (F_2), respectively. Their corresponding orientations were termed as the first principal grip angle (α_1) and the second principal grip angle (α_2). With this terminology, this property can be expressed as follows:

$$\begin{aligned} F_T(\alpha_1) &= 0, & F_N(\alpha_1) &= F_{N_{\max}} = F_1; & F_T(\alpha_2) &= 0, \\ F_N(\alpha_2) &= F_{N_{\min}} = F_2 \end{aligned} \quad (4)$$

Similar to the property shown in Eq. (4), at the maximum and minimum grip tangential forces ($F_{T_{\max}}$ and $F_{T_{\min}}$), the derivative of the grip force ($dF_T/d\alpha$) must be equal to zero.

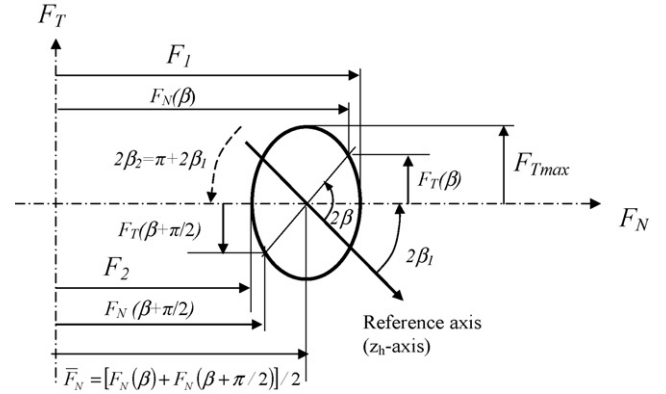


Fig. 2. An ideal ellipse of grip force: F_1 is the first principal (maximum) grip force, which corresponds to the first principal direction ($\beta_1 = \alpha_1 - 90^\circ$); F_2 is the second principal (minimum) grip force, which corresponds to the second principal direction (β_2) and is 90° from the first principal axis; $F_{T_{\max}}$ is the maximum grip tangential force, which is $\pm 45^\circ$ from the principal axes; and \bar{F}_N is the average value of the normal forces in any two orthogonal directions.

If the pressure distribution function is known, according to Eq. (3), the grip normal force at the maximum tangential orientation ($\alpha_{T_{\max}}$) or the minimum tangential orientation ($\alpha_{T_{\min}}$) can be calculated from

$$\begin{aligned} F_N(\alpha_{T_{\max}}) &= R[p(\alpha_{T_{\max}} + \pi) + p(\alpha_{T_{\max}})], \\ F_N(\alpha_{T_{\min}}) &= R[p(\alpha_{T_{\min}} + \pi) + p(\alpha_{T_{\min}})] \end{aligned} \quad (5)$$

Using the above equations, we derived the following theorem (see Appendix A for the detailed derivation): the grip normal and tangential forces form a perfect circle or ellipse on the F_N - F_T plane, as shown in Fig. 2, if the pressure distribution satisfies the following condition:

$$\begin{aligned} p(\alpha) + p\left(\alpha + \frac{\pi}{2}\right) + p(\alpha + \pi) + p\left(\alpha + \frac{3\pi}{2}\right) \\ = \frac{2\bar{F}_N}{R} \equiv \text{constant}, \quad \text{where } \bar{F}_N = \frac{F_1 + F_2}{2} \end{aligned} \quad (6)$$

2.1.3. Hypothesis

Obviously, a uniform pressure distribution ($p = \text{constant}$) satisfies the condition in Eq. (6), which results in a single point on the plane. As also demonstrated in Appendix A, one can create many artificial pressure distribution functions that satisfy Eq. (6) and form their corresponding circles or ellipses. On the other hand, a perfect elliptical pressure distribution on the handle circle does not form a perfect elliptical grip force function because the elliptical pressure function does not satisfy Eq. (6). It is unlikely that the actual grip pressure distribution matches exactly with any of the specific functions that satisfy Eq. (6). Therefore, the actual grip normal and tangential forces will generally not form a perfect circle or ellipse on the F_N - F_T plane.

However, if Eq. (6) is approximately satisfied or the summation of the pressure on any two orthogonal axes varies in a small range, similar to that for an elliptical pressure function,

the two grip force components may form a pattern similar to an ellipse. Therefore, we hypothesized that the idealized grip force applied on a cylindrical handle within a certain range of diameter can be approximately modeled using an elliptical function. Specifically, as shown in Fig. 2, if F_1 , F_2 , F_{Tmax} and β_1 (or α_1) are known, the normal and tangential forces in any direction (β or α) can be estimated from

$$F_N(\beta) \approx F_2 + \frac{F_1 - F_2}{2} [1 + \cos(2\beta - 2\beta_1)] \quad (7)$$

$$F_T(\beta) \approx F_{Tmax} \sin(2\beta - 2\beta_1) \quad (8)$$

The F_2 direction can also be estimated from

$$\beta_2 \approx \beta_1 \pm 90^\circ \quad (9)$$

2.2. Experiments and data analyses

To test the hypothesis, a series of experiments was conducted to measure the grip pressure distributed on a 30 mm handle. Twenty adult subjects (10 females and 10 males) participated in the experiment, some of whose anthropometrics parameters are listed in Table 1.

The grip pressure on the surface of the handle was measured using a resistive flexible pressure mat (111 mm × 111 mm) with 1936 sensor cells (TekScan, Model #5101-100). Each cell dimension is 2.54 mm × 2.54 mm. The sensor mat was first conditioned using a pressure equalizer (NOVEL, 10 bar Pressure Equalizer). Then, it was equalized at 14 pressure levels (0.2, 0.4, 0.6, 0.8, 1.0, 1.4, 1.8, 2.2, 2.6, 3.0, 3.5, 4.0, 5.0, and 6.0 bar). The sensor mat was placed on a flat metal sheet for simulating the handle surface in the equalizing measurements. A fourth order polynomial function (no constant term) was used to fit the equalizing data for each cell. The fit proved to be excellent (mean $r^2 = 0.9986$; and S.D. = 0.0008). The 1936 cell-specific non-linear functions were used to calculate the grip pressure from the data measured in the subject tests.

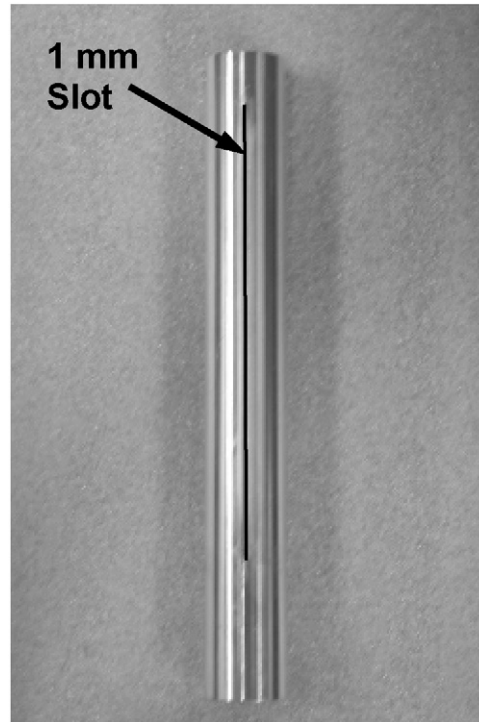


Fig. 3. A view of the handle prior to installation of the pressure sensor mat. In order to prevent sensor cell overlapping and to ensure uniform adhesion to the handle, the edges of the mat were inserted into the 1 mm slot.

A picture of the handle used in this study is shown in Fig. 3. The equalized sensor mat was bonded to the handle surface using a sprayed adhesive. The columns of the sensor elements were aligned longitudinally with the handle. A 1 mm slot was cut along the longitudinal direction of the handle into which the two edges of the sensor mat could be inserted. This slot prevented the overlapping of sensor cells and allowed for uniform adhesion to the handle surface.

After the sensor mat was installed, an in situ check-up test was performed to confirm the calibration factor determined from the equalizer measurement data and to verify the grip

Table 1

Subject anthropometrics (hand length = tip of middle finger to crease at wrist; hand breadth = the width measured at the metacarpals; the hand length or breadth is the average of the values measured on the left and right hands)

Subject	Females				Males			
	Weight (kg)	Stature (m)	Hand length (mm)	Hand breadth (mm)	Weight (kg)	Stature (m)	Hand length (mm)	Hand breadth (mm)
1	49.9	1.67	171	71	74.8	1.79	180	87
2	54.4	1.62	167	74	75.4	1.75	192	87
3	72.5	1.72	169	77	65.0	1.70	174	76
4	56.7	1.60	179	75	102.2	1.73	186	89
5	59.0	1.68	173	76	88.5	1.85	195	93
6	52.0	1.63	180	73	86.2	1.83	185	85
7	54.4	1.61	176	71	74.8	1.75	187	84
8	70.3	1.68	177	74	61.3	1.61	183	73
9	54.7	1.60	172	71	102.1	1.84	195	94
10	58.9	1.68	174	71	79.4	1.75	192	86
Mean	58.3	1.65	174	73	81.0	1.76	187	85
S.D.	7.5	0.04	4	2	13.9	0.07	7	7

force integration algorithm. In this test, one subject pushed (with a grip posture) on the handle fixed on a force measurement device equipped with calibrated force sensors (Interface SMT250). The handle was orientated in three test positions (in the reference axis in Fig. 1, and $\pm 80^\circ$ from the reference axis). Five levels of force from 100 to 500 N were used with two trials per treatment. The 15 pairs of force data obtained from the sensor mat on the handle were found to be highly correlated with the force data measured on the check-up device ($r^2 = 0.9933$). The adjustment to the calibration factors was marginal (4.73%).

As shown in Fig. 4, a power grip posture was used in the measurement. The handle was freely suspended on a string so that the subject could not apply push force to the handle, and the effect of the handle's weight was minimized in the grip pressure measurement. The handle reference axis was aligned with the direction of the z_h -axis of the hand gripping the handle. An adhesive marker was affixed on each hand of each subject to ensure proper hand grip alignment with the reference axis. The hand and arm posture specified in ISO 10819 [14] (90° elbow angle and 0° upper arm angle) was used in the experiment.

Each subject was required to apply two grip force levels: a maximum grip and a medium grip. For the purpose of this study, it was not necessary to precisely control the medium grip force. As a convenient approach, the medium grip force was determined by taking half of the maximum pressure observed in a subject training trial. As presented in the next section, the average medium grip force was about 40% of the average maximum grip force. When the specified gripping force was stable, the pressure data were recorded for 3 s at a sampling rate of 5 Hz for a total of 15 frames of data per trial. Two trials were performed for each test treatment. After each trial, the subject rested for 3 min. Both hands were used in the experiment; each subject alternated between left-hand and right-hand grip trials. The sequence of the test treatments for each hand was randomized for each subject. The tare values of the sensor cells were recorded before and after each subject test.

The 15-frame data for each sensor element were averaged to represent the raw pressure value for each trial. The average tare value of each sensor cell was subtracted from the raw pressure value to obtain the pure grip pressure. The data for each column of 44 cells were summed to represent the

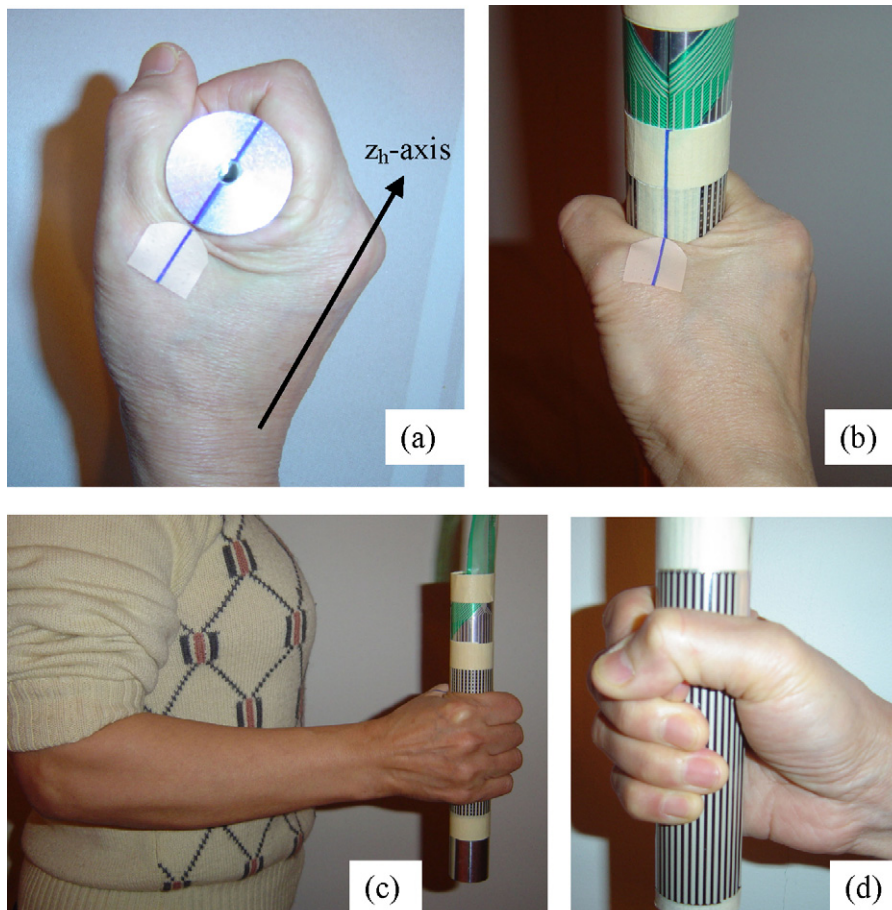


Fig. 4. Test setup and the hand–arm posture used in the experiment: (a) the handle reference axis is aligned with the z_h -axis of the hand biodynamic coordinate system to determine the marker position on the hand; (b) the marker on the hand is aligned with that on the instrumented handle to ensure that a consistent hand grip orientation is achieved; (c) hand and arm posture used in the experiment; and (d) a side view of the hand grip posture.

pressure (p) for each step (9.67°) of the integration around the handle circle. The grip pressure on the two halves of the handle was separately integrated according to Eq. (1), which resulted in two values of opposing grip forces in each measurement axis. These two values were averaged, and the result was used to represent the final grip force as a function of the measurement axis.

The elliptical model expressed in Eqs. (7) and (8) was used to fit each of the 160 pairs of data (20 subjects, 2 hands, 2 grip levels, 2 trials) to test the hypothesis. The correlation coefficient (r^2 -value) for each fit was calculated and used to evaluate the model. Paired t -tests were used wherever applicable.

3. Results

Fig. 5 shows an example of the distribution of the contact pressure per unit length around the handle circumference measured with the right hand of a subject. The maximum peak pressure is about 80° from the z_h -axis, which is in range of the angular positions of the middle and distal phalanges (also see Fig. 4a and d). The pressure distribution pattern at the finger side is different from that at the palm side.

Fig. 6 shows the two grip force functions on the opposite sides of the cylindrical handle, together with their mean value. They are integrated from the pressure function shown in Fig. 5. The data for the two sides are marginally different (the maximum normal force difference = 8.9%) but their basic trends remain the same. The first principal/maximum normal grip force is also in the range of the angular positions of the middle and distal phalanges, similar to that shown in Fig. 5. Unless otherwise specified, the mean grip force functions are used in the following presentations.

The average pressure functions measured at the maximum grip level and the medium grip level are shown in Figs. 7 and 8, respectively. As expected, the pressure measured with the male subjects is generally higher than that measured with the female subjects. Similar to that shown in Fig. 5, the maximum peak pressure in each case is in the range of the angular positions of the middle and distal phalanges. The z_h -axis is in the low pressure zone in all the cases.

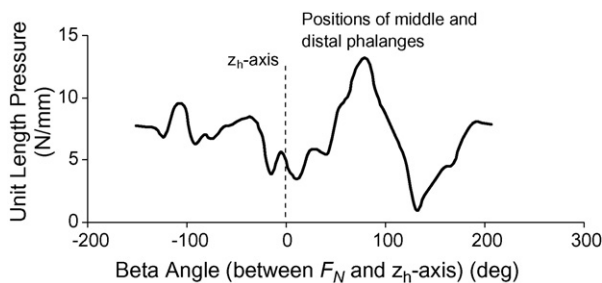


Fig. 5. An example of the pressure distribution as a function of beta angle (β).

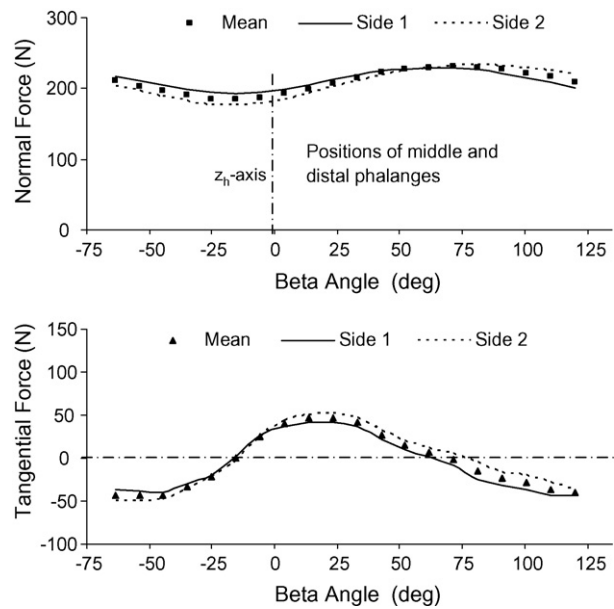


Fig. 6. Examples obtained from a female subject of grip force values on opposing halves of the 30 mm handle and their mean value as functions of beta angle (β) measured from the reference axis (z_h -axis), which are integrated from the pressure function shown in Fig. 5.

The average grip force functions shown in Figs. 9 and 10 are calculated using the pressure functions shown in Figs. 7 and 8, respectively. Similar to that shown in Fig. 6, the grip force data on the two opposite sides of the handle are marginally different. The maximum difference between the two normal forces is between 3.1 and 7.4% in five of the eight cases, and between 10.6 and 13.2% in the remaining three cases. Fig. 9 shows the mean grip force functions of the two grip force components at the maximum grip level, together with the modeling results. Fig. 10 shows those at the medium grip level. The maximum difference between the modeling results and the experimental data of the grip normal force is less than 3.6%. Consistent with the hypothesis, the normal and tangential forces form a pattern similar to an ellipse in each case. At the minimum and maximum normal forces, the tangential force goes to zero. The difference between the angles of the peak (principal force F_1) and valley (principal force F_2) grip normal force values is approximately 90° . The orientation of the first principal grip force (β_1) in each case is also close to the angular position of the maximum peak in the corresponding pressure function shown in Figs. 7 and 8.

The elliptical model was further used to fit each pair of experimental data. Table 2 lists the correlation statistics for the model for all the 160 pairs of experimental data. Even in the worst case, the predicted grip normal force is still highly correlated with the experimental data ($r^2 = 0.9659$). Judging from these 160 pairs of r^2 -values, the elliptical model generally fits the normal component better than the tangential component (t -test, $p_r < 0.001$). This difference can also be seen in Figs. 9 and 10.

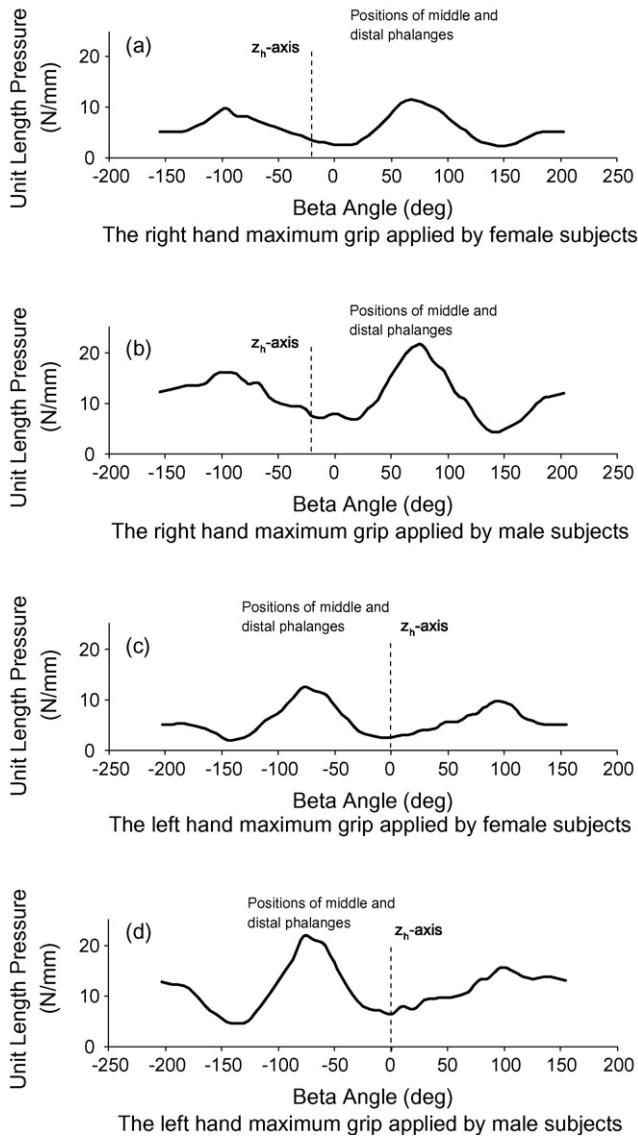


Fig. 7. Average pressure distributions as functions of β angle at the maximum grip level.

Table 2
Correlations (r^2 -values) between the model and the 160 sets of experimental data

Parameters	Maximum grip force level		Medium grip force level	
	Right hand	Left hand	Right hand	Left hand
Normal force component (F_N)				
Mean	0.9942	0.9913	0.9934	0.9906
S.D.	0.0049	0.0049	0.0038	0.0074
Maximum	0.9986	0.9982	0.9984	0.9988
Minimum	0.9706	0.9738	0.9844	0.9659
Tangential force component (F_T)				
Mean	0.9728	0.9565	0.9670	0.9525
S.D.	0.0260	0.0242	0.0216	0.0311
Maximum	0.9927	0.9875	0.9917	0.9871
Minimum	0.8525	0.8781	0.9187	0.8592

The effect of the test sequence on the principal directions in all four test treatments (left hand maximum grip, right hand maximum grip, left hand medium grip, and right hand medium grip) is not significant ($p_r \geq 0.193$). The effect of the test sequence on the principal forces is also generally insignificant ($p_r \geq 0.296$) except in the principal force of the right hand maximum grip ($p_r = 0.033$). There is a large variation of the principal grip force direction among the subjects. The first principal angle ($\beta_1 = 83.3^\circ$) of the female subjects is generally greater than that (73.3°) of the male subjects ($p_r = 0.010$). However, the correlation between hand length and the principal angle is very poor; likewise, that between hand breadth and the principal angle is also very poor. These relationships are depicted in Fig. 11.

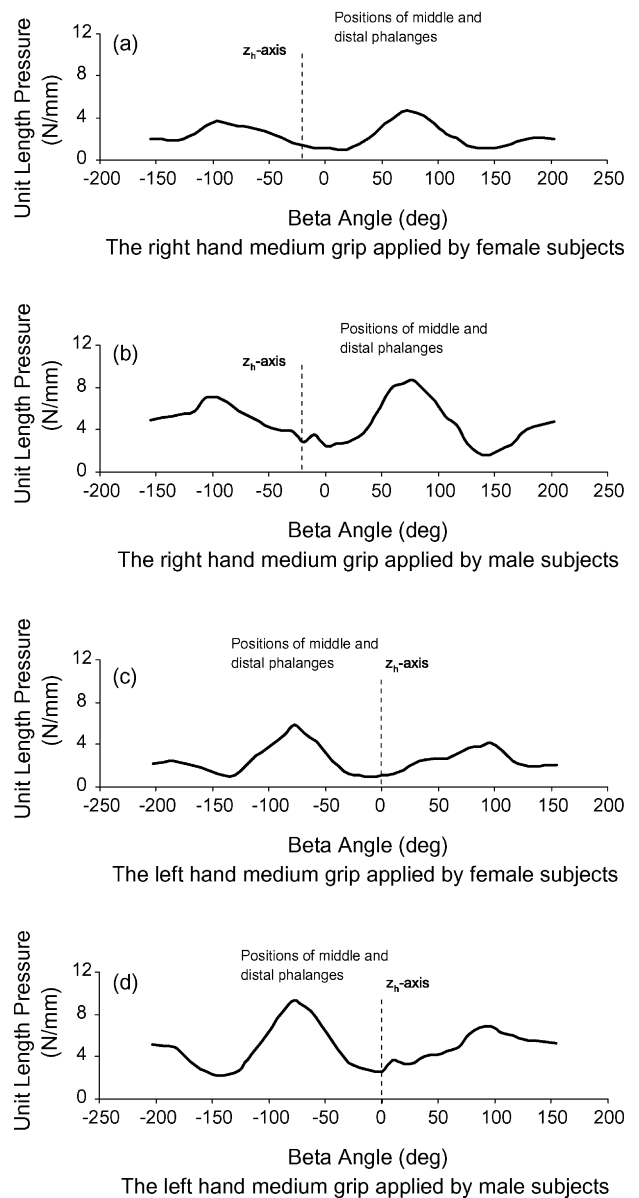


Fig. 8. Average pressure distributions as functions of β angle at the medium grip level.

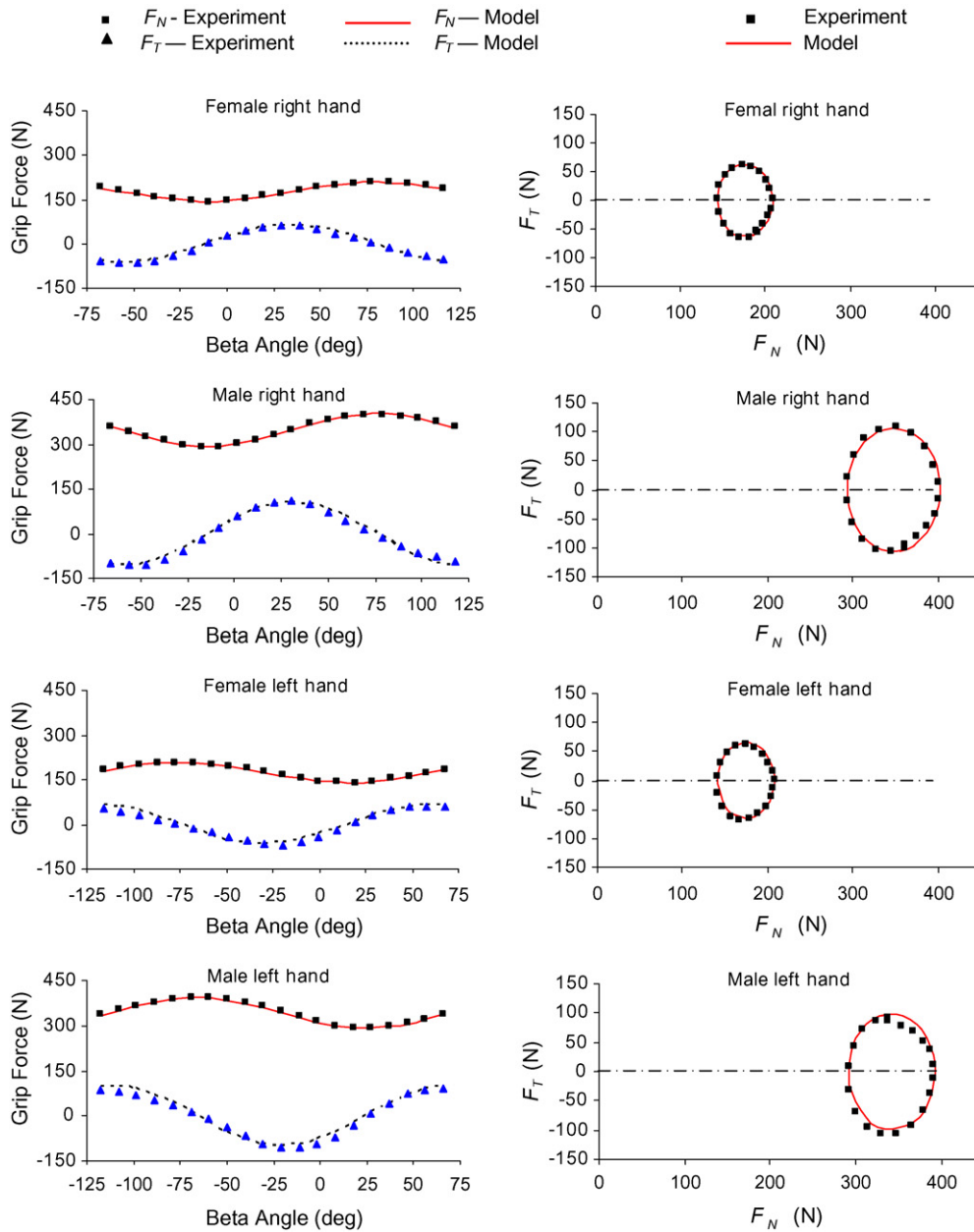


Fig. 9. Comparisons of the elliptical modeling and the experimental data measured at the maximum grip force level.

As listed in Table 3, the average principal angle (β_1) is about 78.3° measured from the z_h -axis of the biodynamic coordinate system defined in ISO 8727 [1]. The first principal angle (76.8°) at the right hand is not significantly

different from that (79.7°) at the left hand ($p_r = 0.106$). The principal angle (76.1°) under the maximum grip action is marginally less than that (80.5°) under the medium grip action ($p_r < 0.001$). However, the two angles are correlated, as shown in Fig. 12.

Table 3
The first principal/maximum force angle (β_1)

Parameters	Maximum grip force level		Medium grip force level	
	Right hand	Left hand	Right hand	Left hand
Mean ($^\circ$)	75.5	76.7	78.2	82.8
S.D. ($^\circ$)	12.5	14.8	11.5	15.0
Maximum ($^\circ$)	99.9	110.4	99.9	117.8
Minimum ($^\circ$)	54.4	47.1	56.5	48.3

The mean value of the first principal/maximum grip forces measured at the maximum grip force level for the male subjects (402 N) is almost twice that for the female subjects (210 N) ($p_r < 0.001$). Other principal force data are listed in Table 4. These data also reveal substantial inter-subject variation. On average, the first principal force is more than 40% larger than the second principal force ($p_r < 0.001$). These two principal forces are highly correlated, as shown in Fig. 13. In the case of the maximum grip force level, the regression

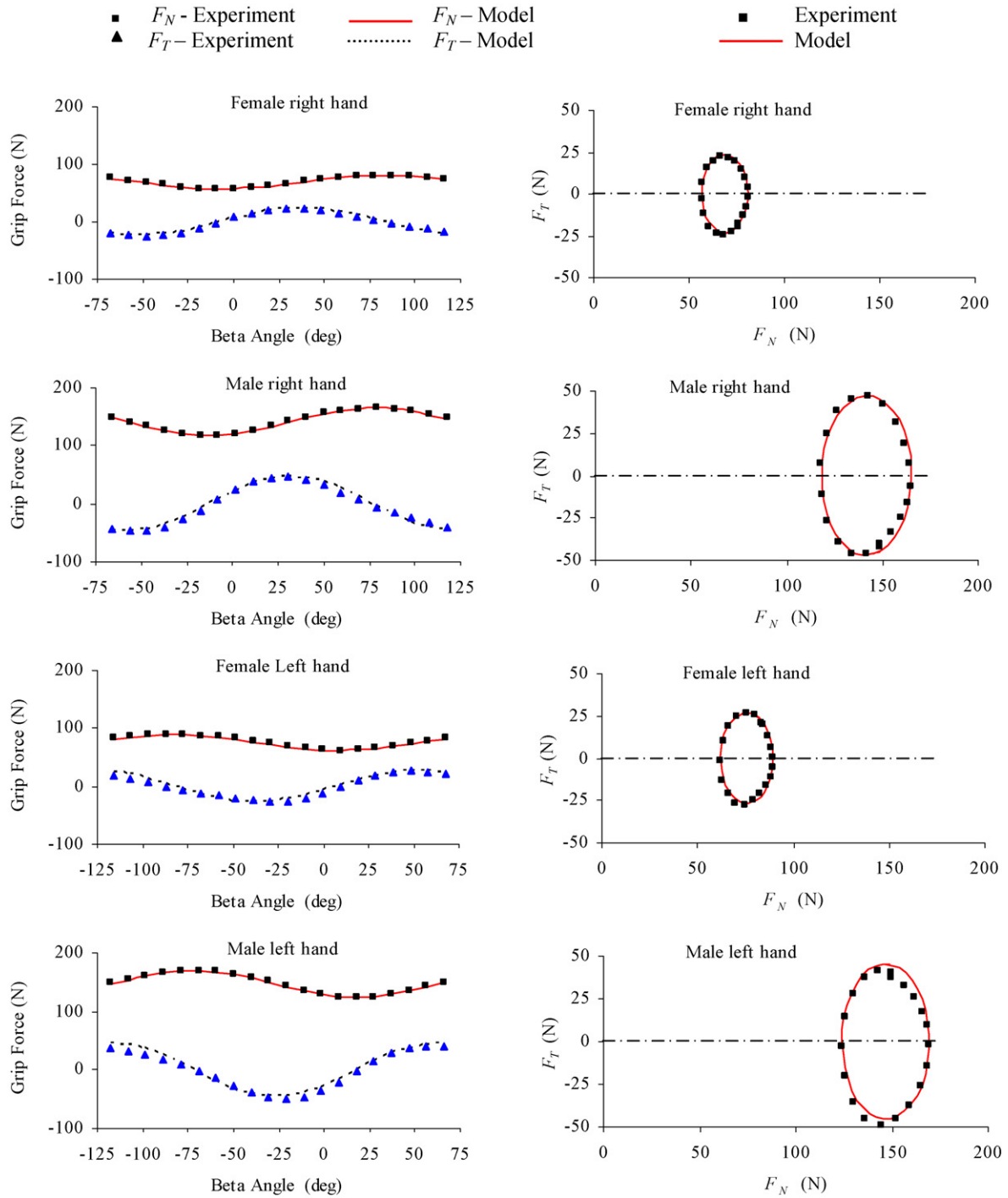


Fig. 10. Comparisons of the elliptical modeling and the experimental data measured at the medium grip force level.

Table 4
The principal grip forces (F_1 = maximum, F_2 = minimum) for each hand at each force level

Parameters	Maximum grip force level				Medium grip force level			
	F_1		F_2		F_1		F_2	
Hand	Right	Left	Right	Left	Right	Left	Right	Left
Mean (N)	308	304	214	211	124	131	86	91
S.D. (N)	146	151	107	109	67	66	51	48
Maximum (N)	623	652	462	457	319	314	247	236
Minimum (N)	133	101	87	75	35	57	24	33

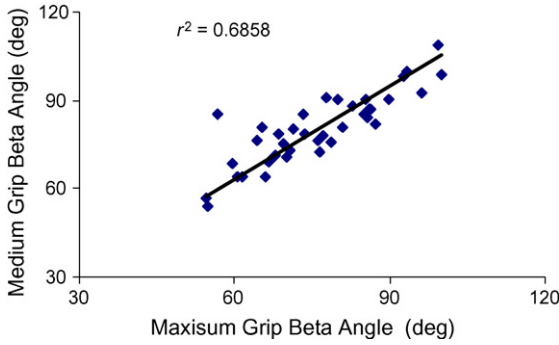


Fig. 11. Correlation between the first principal angles measured under the maximum and medium grip actions.

relationship is expressed as follows:

$$F_1 = 1.4203 F_2 \tag{10}$$

In the case of the medium grip force level, the regression relationship is very similar to that for the maximum grip force level, which is expressed as follows:

$$F_1 = 1.4132 F_2 \tag{11}$$

Consequently, the first principal force is highly correlated to the mean value (F_{mean}) of the two principal forces ($r^2 = 0.9953$), which can be estimated from

$$F_{\text{mean}} = \frac{F_1 + F_2}{2} = 0.8493 F_1 \tag{12}$$

The first principal force is also highly correlated to the square-root value (F_{sqr}) of the two principal forces ($r^2 = 0.9970$), which is the magnitude of the vector defined in a previous study [15]. This measure can be estimated from

$$F_{\text{sqr}} = \sqrt{F_1^2 + F_2^2} = 1.221 F_1 \tag{13}$$

Table 5 lists the data for comparing the maximum tangential force with the difference between the two principal grip normal forces ($F_1 - F_2$). As indicated, the maximum tangential force and the principal force difference are similar. The maximum tangential force mean values for each of the four test treatments are not statistically different from those of the principal force differences ($p_r \geq 0.240$). As shown in Fig. 14, the maximum tangential force is highly correlated ($r^2 = 0.9960$) with the principal force difference. Their regression relationship is expressed as follows:

$$F_{T\text{max}} = 1.0035(F_1 - F_2) \tag{14}$$

As shown in Fig. 15, as the first principal force applied to the 30 mm handle increases, the difference between the two principal forces generally increases ($r^2 = 0.8553$). Because the two principal grip forces are highly correlated, increasing the second principal force also generally increases the principal force difference ($r^2 = 0.7203$). Because the principal force difference is highly correlated to the maximum tangential force, increasing the principal forces also generally increases the maximum tangential force ($r^2 \geq 0.7465$).

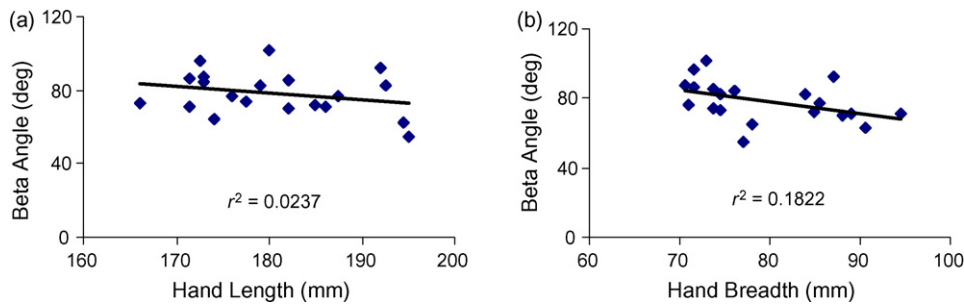


Fig. 12. Correlations (a) between the first principal angle (β_1) and hand length and (b) between the first principal angle (β_1) and hand breadth.

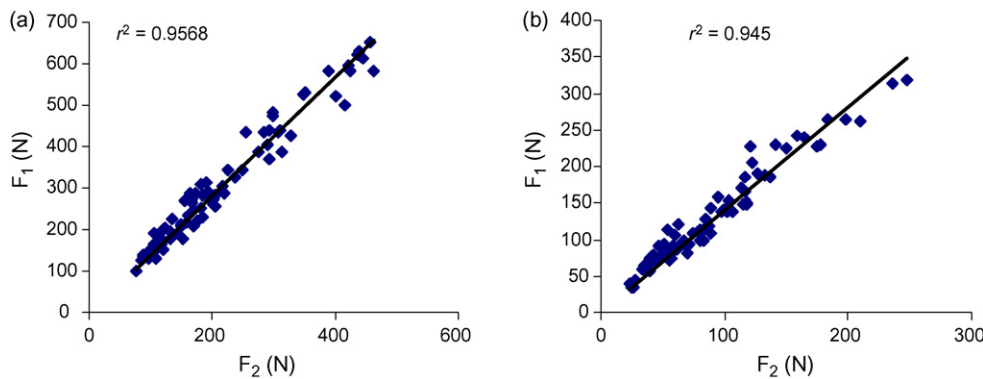
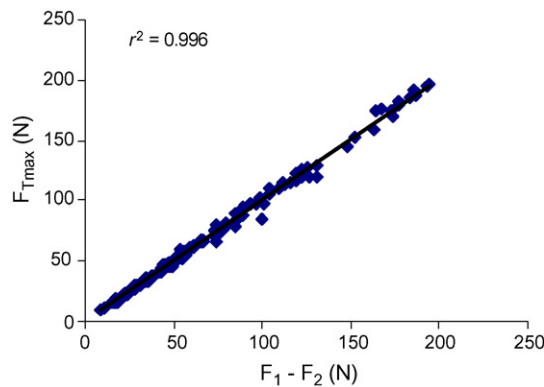
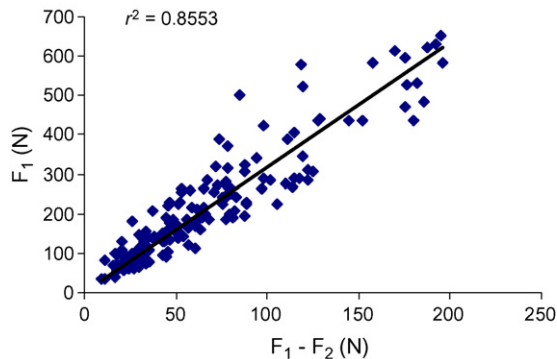


Fig. 13. Correlation between the first principal/maximum grip force and the second principal/minimum grip force at (a) the maximum grip force level and (b) the medium grip force level.

Table 5

Comparison of the maximum grip tangential force (F_{Tmax}) and the difference between the principal forces ($F_1 - F_2$)

Parameters	Maximum grip force level				Medium grip force level			
	F_{Tmax}		$F_1 - F_2$		F_{Tmax}		$F_1 - F_2$	
Hand	Right	Left	Right	Left	Right	Left	Right	Left
Mean (N)	94	92	94	93	38	41	38	41
S.D. (N)	46	48	45	49	21	21	21	21
Maximum (N)	194	193	196	195	104	85	106	83
Minimum (N)	27	21	27	21	9	17	9	16

Fig. 14. Correlation between the maximum grip tangential force and the difference between the two principal forces ($F_1 - F_2$).Fig. 15. Correlation between the first principal/maximum grip force (F_1) and the difference between the two principal forces ($F_1 - F_2$).

4. Discussion

This study confirmed that a grip force measurement generally depends on the orientation of the measurement axis and that the maximum value can be significantly different from the minimum value in a given gripping action. The results of this study also demonstrated that the grip force applied to a 30 mm handle can be reasonably described using an elliptical model. This study also identified the principal directions of grip forces applied to this handle and their fundamental characteristics. Although further studies are required to determine the range of the handle diameters applicable to the model, this study initiated a new approach to characterize the grip force.

This elliptical model and its features identified in this study provide a clearer picture of the characteristics of grip forces

applied to 30 mm handles. A cylindrical grip strength meter that is developed based on the proposed theory could provide more information regarding grip strength than does the Jamar dynamometer. According to Eq. (7), determinations of principal grip force magnitudes and directions generally require measuring the normal force in at least three independent directions. For example, the normal force can be measured on three axes that are 120° apart from each other. Because the maximum tangential force is highly correlated with the difference between the principal forces, as shown in Fig. 14, the relationship expressed in Eq. (14) may be used to estimate the principal force magnitudes and directions by measuring the tangential force. However, the results of this study suggest that the measurement of the tangential force is not as reliable as that of the normal force. This is because the tangential force is relatively small and is more sensitive to measurement error or ‘noise’ than is the normal force. The tangential force may become less reliable when the grip pressure is more uniformly distributed. Furthermore, the tangential force is usually not important for practical applications. Therefore, it is better to construct the ellipse of grip force by measuring the normal force values in more than two directions. The 30 mm dynamometer proposed by Chadwick and Nicol [17] may be applied to simultaneously measure the normal force values in three directions in a gripping action and can be used to estimate the principal forces and directions.

This study found that the average direction of the first principal grip force on the 30 mm handle is about 78° from the z_h -axis defined in ISO 8727 [1] or ISO 5349-1 [16]. This means that the z_h -axis is much closer to the minimum grip direction. As shown in Figs. 7 and 8, the grip pressure in the neighborhood of the z_h -axis is also close to the lowest level. Therefore, the results of this study do not support that “the direction of the main grip force is generally parallel to the z -axis” as stated in ISO 15230 [4].

The two force values used to form Edgren et al.’s grip force vector were measured on two specific orthogonal axes of the hand [15]. According to the proposed ellipse model, the two normal forces, defined as $F_N(\alpha)$ and $F_N(\alpha + \pi/2)$ in Fig. 2, are approximately opposite each other on the ellipse. If the two orthogonal axes are in the maximum and minimum orientations, respectively, the corresponding two forces are, respectively, the first and second principal forces. Obviously, the angle of the vector formed with these two forces is not in the principal grip direction. Only when the two normal force values are equal to each other, which results in 45° , does the

vector direction coincide with the direction of the principal grip force. Furthermore, the magnitude of the vector is not equal to the grip force value in any direction. Therefore, in a general case, Edgren et al.'s grip force vector does not provide information on the maximum grip force and its direction. It is better to use the proposed principal force approach for understanding and characterizing the grip force applied on a cylindrical handle.

As observed in this study, the principal direction seems to be related to the position of the fingers on the handle, probably because the maximum pressure can be generally found at the fingertips [10] or in the position range of distal and middle phalanges, as observed in this study. Therefore, the principal grip direction is likely to be a function of handle diameter and its subsequent effect on the finger position. This suggests that the grip forces measured by traditional means on two handles with different diameters in the same orientation may not be generally comparable. The principal grip force is a reasonable measure to use when comparing gripping efforts applied to differently-sized handles.

As also observed in this study, the principal grip directions remain practically the same for gripping actions at maximum and medium grip force levels, which suggests that the magnitude of the grip force on the same handle does not substantially influence the principal grip force direction. If the measurement reference axis used when monitoring and controlling the grip force in an experiment is fixed for all the subjects, which is required in the ISO glove test [14] and the biodynamic tests, e.g., [12,13], the statistical relationship between the principal force and the force measured in relation to the measurement axis is also consistent if the same sized handle is used. In such a case, the average force measured in one lab may be comparable with that measured in another lab if the number of the subjects is sufficiently large.

However, if the grip effort of each individual or a specific group of population is of concern, the single-axis method may bring a bias in the measurement. As shown in Table 3, there was a large inter-subject variation in the principal direction data. Because of this variation, the grip force values measured on the same handle in the same direction with different subjects may not be directly comparable. As also observed in this study, the average principal angle (83.3°) of the female participants is larger than that of the male participants (73.3°). One of the possible explanations may be that the male hands are generally longer than female hands as shown in Table 1; for males, the thumb generally wraps further around the handle than it does for females, thus the principal angle is shifted closer to the z_h -axis. However, the male subjects' other four fingers also generally wrap further in the opposite direction around the handle than those of the female subjects. Therefore, the effects of the finger positions on the principal angle are complex. The poor correlation between hand length and the principal angle, as shown in Fig. 11, suggests that there are factors other than hand dimensions that influence the principal grip direction. The principal direction may also depend on an individual's gripping habits; some subjects tended to

apply more force at the fingertips than others. This may be a more reasonable explanation on why these specific female participants had a different principal grip direction from the male subjects. Whereas further studies are required to confirm the difference between the female and male principal angles and to further identify the influencing factors, the above observations suggest that like the magnitude of the principal grip strength, the principal grip direction is also individual-specific. Therefore, to compare or control the grip effort among individuals or different population groups, the principal grip force is more reliable than the single-axis grip force.

A previous study reported the relationship between a single-axis grip force and the total contact force [9]. In accordance with the above discussions, such a formula may become invalid if the single-axis grip force is measured in a different axis than that used in the reported study, because the relationship could change with a variation in grip orientation. The elliptical model can be used to help appropriately apply the formula or to modify the formula when the single-axis force is measured in a different axis.

According to Eq. (2), the two values of the idealized grip force measured on the two halves of the handle are theoretically the same. However, the results of this study show that they could be marginally different, as shown in Fig. 6. This is likely because (a) the friction force, especially on the distal phalanx, may be influential, as Amis [18] argued; (b) the handle weight and initial handle force may come into play in some of the tests; and (c) some measurement errors through the use of the flexible sensor mat are unavoidable. The averaging process may reduce the influences of these factors. The characterization of the grip force can be improved when a more reliable measurement method and more information on these influencing factors are available. Nevertheless, despite of the presence of these error sources, the overall comparisons of the theoretical predictions and the experimental data are still very reasonable, especially the normal force that is practically useful. This suggests that the ellipse model reflects the dominant features of the grip force function, and it is fairly robust, at least when applied to the 30 mm handle.

5. Conclusions

In this study, the idealized grip force applied to a cylindrical handle was described using a normal component and a tangential component calculated from the grip pressure vertical to the handle surface. This study developed basic formulas describing the idealized grip force and identified the fundamental properties of such a grip force. These properties are generally applicable to the idealized grip force applied to any cylindrical handle.

This study concluded that grip forces applied to 30 mm handles can be approximately described using an elliptical model. This is especially true of the normal component that is conventionally termed as grip force and used in many prac-

tical applications. Further studies are required to determine the range of handle sizes to which the elliptical model can be appropriately applied.

This study confirmed that the single-axial grip force is generally insufficient to represent a gripping effort applied to a cylindrical handle; alternatively, we proposed that grip forces can be better described using principal forces and orientations. This study found that the first principal/maximum grip direction for a grip force applied to a 30 mm handle is about 78° from the z_h -axis of the biodynamic hand coordinate system defined in ISO 8727 [1] or ISO 5349-1 [16]. The second principal/minimum grip axis is about 90° from the first principal axis. The maximum grip force is highly correlated to the minimum grip force, but the former is generally about 1.42 times the latter. Both the maximum and minimum grip forces are highly correlated to their difference as well as to the maximum tangential component. For the handle used in this study, the difference between the two extreme forces is generally equal to the maximum tangential component.

Appendix A

Differentiating Eq. (1) with respect to α results in the following relationship:

$$\begin{aligned} \frac{dF_N(\alpha)}{d\alpha} &= R \int_0^\pi p'(\alpha + \theta) \sin(\theta) d\theta \\ &= R \int_0^\pi \sin(\theta) dp(\alpha + \theta) = R[\sin(\theta)p(\alpha + \theta)]_0^\pi \\ &\quad - R \int_0^\pi p(\alpha + \theta) \cos(\theta) d\theta \\ &= -R \int_0^\pi p(\alpha + \theta) \cos(\theta) d\theta = -F_T(\alpha) \end{aligned} \quad (A1)$$

The condition for $F_N(\alpha)$ to reach the maximum is

$$\frac{dF_N(\alpha)}{d\alpha} = 0, \quad \text{or} \quad F_T(\alpha) = 0 \quad (A2)$$

Similarly,

$$\begin{aligned} \frac{dF_T(\alpha)}{d\alpha} &= R \int_0^\pi p'(\alpha + \theta) \cos(\theta) d\theta \\ &= -R[p(\alpha + \pi) + p(\alpha)] + F_N(\alpha) \end{aligned} \quad (A3)$$

The condition for $F_T(\alpha)$ to reach the maximum is

$$\frac{dF_T(\alpha)}{d\alpha} = 0, \quad \text{or} \quad F_N(\alpha) = -R[p(\alpha + \pi) + p(\alpha)] \quad (A4)$$

If the grip normal and tangential forces can be represented by a symmetrical, closed loop (i.e., a circle or an ellipse) on a plane defined by the F_N – F_T coordinate system in similar fashion to Mohr's circle of stress used in the mechanics of materials [19], for any α , the normal forces satisfy the

following condition:

$$\frac{F_N(\alpha) + F_N(\alpha + \pi/2)}{2} = \frac{F_1 + F_2}{2} = \bar{F}_N = \text{constant} \quad (A5)$$

where \bar{F}_N is the average grip normal force.

Differentiation of Eq. (A5) with respect to α results:

$$F'_N(\alpha) + F'_N\left(\alpha + \frac{\pi}{2}\right) = 0 \quad (A6)$$

Substitution of Eqs. (A1)–(A6) results in the relationship:

$$F_T(\alpha) = -F_T\left(\alpha + \frac{\pi}{2}\right) \quad (A7)$$

This condition is consistent with the circle or ellipse hypothesis. By further differentiating Eq. (A7) with respect to α and using the relationships of Eqs. (A3) and (A5), the dependence of the normal force on the contact pressure at the characteristic points is derived:

$$\begin{aligned} F_N(\alpha) + F_N\left(\alpha + \frac{\pi}{2}\right) &= R \left[p(\alpha) + p\left(\alpha + \frac{\pi}{2}\right) + p(\alpha + \pi) \right. \\ &\quad \left. + p\left(\alpha + \frac{3\pi}{2}\right) \right] = 2\bar{F}_N = \text{constant} \end{aligned} \quad (A8)$$

For a uniformly distributed pressure, i.e., $p(\alpha) = \text{constant}$, Eq. (A8) is perfectly satisfied. In this particular case, the circle or ellipse shrinks to a point.

Many pressure distribution functions that satisfy Eq. (A8) can be created. An example is a sine-like distribution, given as follows:

$$\begin{aligned} p(\alpha) &= p(\alpha + \pi), \quad p\left(\alpha + \frac{\pi}{2}\right) = p\left(\alpha + \frac{3\pi}{2}\right), \\ p(\alpha) &= p_0 \sin(\alpha + \theta) \quad 0 \leq (\alpha + \theta) < \frac{\pi}{2}, \\ p\left(\alpha + \frac{\pi}{2}\right) &= p_0[1 - \sin(\alpha + \theta)] \end{aligned} \quad (A9)$$

where p_0 is a constant.

References

- [1] ISO 8727. Mechanical vibration and shock – human exposure – biodynamic coordinate systems. Geneva, Switzerland: International Organization for Standardization; 1997.
- [2] NIOSH. Musculoskeletal disorders and workplace factors: a critical review of epidemiologic evidence for work-related musculoskeletal disorders of the neck, upper extremity, and low back. Cincinnati, OH: NIOSH Publication 97-141. U.S. Department of Health and Human Services, National Institute for Occupational Safety and Health; 1997.
- [3] Sande LP, Coury HJCG, Oishi I, Kumar S. Effect of musculoskeletal disorders on prehension strength. *Appl Ergon* 2001;32:609–19.
- [4] ISO/DIS 15230. Mechanical vibration and shock—coupling forces at the machine–man interface for hand-transmitted vibration. Geneva, Switzerland: International Organization for Standardization; 2005.
- [5] Josty IC, MacQuillan AHF, Murison MSC. Functional outcomes following surgical repair of wrist extensor tendons. *Br J Plastic Surg* 2003;56:120–4.

- [6] Kwok TG, Huang CH, Kao HC. Endoscopic carpal tunnel release using a new median nerve protector. *Arthrosc J Arthrosc Relat Surg* 2004;20:841–7.
- [7] Färkkilä M, Aatola S, Starck J, Korhonen O, Pyykkö I. Hand-grip force in lumberjacks: two-year follow-up. *Int Arch Occup Environ Health* 1986;58:203–8.
- [8] Abbott JH, Patla CE, Jensen RH. The initial effects of an elbow mobilization with movement technique on grip strength in subjects with lateral epicondylalgia. *Man Ther* 2001;6:163–9.
- [9] Welcome DE, Rakheja S, Dong RG, Wu JZ, Schopper AW. An investigation on the relationship between grip, push, and contact forces applied to a tool handle. *Int J Ind Ergon* 2004;34:507–18.
- [10] Aldien Y, Welcome DE, Rakheja S, Dong RG, Boileau PE. Contact pressure distribution at hand–handle interface: role of hand forces and handle size. *Int J Ind Ergon* 2005;35:267–86.
- [11] McDowell TW, Wiker SF, Dong RG, Welcome DE, Schopper AW. Evaluation of Psychometric Estimates of Vibratory Hand-Tool Grip and Push Forces. *Int J Ind Ergon* 2006;36:119–28.
- [12] Dong RG, Schopper AW, McDowell TW, Welcome DE, Wu JZ, Smutz WP, et al. Vibration energy absorption (VEA) in human fingers–hand–arm system. *Medical Engineering and Physics* 2004;26:483–92.
- [13] Marcotte P, Aldien Y, Boileau PE, Rakheja S, Boutin J. Effect of handle size and hand–handle contact force on the biodynamic response of the hand–arm system under Z_h -axis vibration. *J Sound Vibration* 2005;283:1071–91.
- [14] ISO 10819. Mechanical vibration and shock – hand–arm vibration – method for the measurement and evaluation of the vibration transmissibility of gloves at the palm of the hand. Geneva, Switzerland: International Organization for Standardization; 1996.
- [15] Edgren CS, Radwin RG, Irwin CB. Grip force vectors for varying handle diameters and hand sizes. *Hum Factors* 2004;46:244–51.
- [16] ISO 5349-1. Mechanical vibration – measurement and evaluation of human exposure to hand-transmitted vibration – part 1: general requirements. Geneva, Switzerland: International Organization for Standardization; 2001.
- [17] Chadwick EKJ, Nicol AC. A novel force transducer for the measurement of grip force. *J Biomech* 2001;34:125–8.
- [18] Amis AA. Variation of finger forces in maximal isometric grasp tests on a range of cylinder diameters. *J Biomed Eng* 1987;9:313–20.
- [19] Blake A. Practical stress analysis in engineering design. New York: Marcell Dekker; 1990.